Mon. Not. R. astr. Soc. (1990) **244**, 458–464

Dust around H II regions – II. W49A

D. Ward-Thompson and E. I. Robson
School of Physics and Astronomy, Lancashire Polytechnic, Preston PR1 2TQ

Accepted 1989 December 12. Received 1989 November 7

SUMMARY

Submillimetre continuum maps, and *IRAS* calibrated raw data maps, on which a new 'destriping' technique has been used, are presented of W49A, showing extensive emission from cool dust in the region. The dust emission is fitted by a greybody function with a temperature of 50 K and submillimetre spectral index $\beta = 1.8 \pm 0.2$, consistent with previous work. The cloud is shown to be optically thin at wavelengths longer than 150 μm, so the submillimetre fluxes can be used to estimate the total dust mass, which is found to be 2400 $M_\odot$. The 'filling factor' implies that the dust cloud is highly fragmented on small scales, possibly indicating continuing star-forming activity. The total far-infrared luminosity of the cloud is found to be 2.7×10^7 $L_\odot$, making W49A one of the most luminous star-forming regions in the Galaxy. The morphology of the cloud is diagnosed as consisting of an association of H II regions surrounded by a dust cloud composed of grains at two characteristic temperatures.

1 INTRODUCTION

The W49 dark cloud lies at a distance of 13.8 ± 0.8 kpc (Reifenstein *et al.* 1970), and is a highly complex, and much studied region consisting of two main components – W49A and W49B. W49B is a massive supernova remnant (Clegg, Rowan-Robinson & Ade 1976). W49A contains three separate far-infrared peaks, referred to as W49NW, W49SE and W49SW (Harvey, Campbell & Hoffmann 1977). W49NW is more usually referred to as W49N (e.g. Dreher *et al.* 1984), and this is the convention we shall adopt in this paper. W49N itself contains a number of embedded infrared sources (Becklin, Neugebauer & Wynn-Williams 1973), OH masers (Gaume & Mutel 1987), highly luminous H_2O masers (Genzel *et al.* 1978), and a cluster of compact H II regions (Dreher *et al.* 1984).

W49N is coincident with radio source number 4 of Wynn-Williams (1971), which was seen in the radio continuum by van Gorkom *et al.* (1980), although they did not detect it in the H109α recombination line. W49N is also located in the central zone of a high-velocity CO outflow (Scoville *et al.* 1986). The exciting source of this outflow is difficult to identify due to the distance and compactness of the object, and in fact could be associated with any of the seven H II regions of Dreher *et al.* (1984).

All of these observations show that W49 is an intensely active region of recent massive star formation. To examine the overall structure of dust in this cloud, Calibrated Raw Detector Data (CRDD) from the *IRAS* satellite (Neugebauer *et al.* 1984) were obtained, as well as higher resolution maps at submillimetre wavelengths. The *IRAS* raw data present a unique opportunity to study the large-scale distribution of far-infrared emission from a region, since the resolution is almost an order of magnitude greater than the *SKYFLUX* maps, and flux measurements of small extended regions are more accurate than can be obtained from the *Point Source Catalog*. This work is part of an ongoing programme of investigation of H II regions, to measure properties such as mass, temperature and degree of fragmentation of dust in the dense cores of dark clouds.

2 OBSERVATIONS

IRAS (Neugebauer *et al.* 1984) Calibrated Raw Detector Data (CRDD) were obtained from the Rutherford Appleton Laboratory (RAL) for a 2×2 deg^2 field centred on W49 to ensure an accurate background subtraction. This was carried out in the manner pioneered in association with the STARLINK *IRAS* Applications Programmer and described by Ward-Thompson *et al.* (1989), hereafter referred to as Paper I. Briefly, the procedure employed an iterative method to fit a polynomial of specified order (in this case a straight line) to the background sky, which was then interpolated across the object and subtracted. No colour corrections (IRAS *Explanatory Supplement* 1984) were applied to the maps. *IRAS* Low Resolution Spectrograph (LRS) data were obtained from the STARLINK Database MicroVax of RAL. Standard STARLINK software was used for all data reduction, which was carried out on the Lancashire Polytechnic MicroVax minor node of the UK STARLINK network.

Submillimetre data were obtained at UKIRT on 1988 January 7, 8 and 11 (350, 800 and 1100 μm, respectively),

using the common-user millimetre/submillimetre photometer UKT 14 (Duncan *et al.* 1990), calibration being made with respect to the planet Mars. Apertures of 25, 50 and 63 arcsec were used at 350, 800 and 1100 μm, respectively, using a chop throw of 150 arcsec in RA in each case. Maps were made with a step size equal to half the aperture diameter at each wavelength, ensuring that each map was fully sampled. Single-point beam-switched photometry was also performed at 350, 800 and 1100 μm on each date using a 63-arcsec aperture and a 150-arcsec chop throw in RA.

3 *IRAS* RESULTS

Fig. 1(a–d) shows isophotal contour maps of the W49 region at 12, 25, 60 and 100 μm. A bright, slightly extended source, marked with a cross, can be seen in all four wavebands at the position of W49A (Clegg, Rowan-Robinson & Ade 1976), which is listed in the IRAS *Point Source Catalog* as 19078+0901. The point spread functions of the *IRAS* detectors have not resolved the three components of W49A – namely W49N, W49SW and W49SE – which were clearly

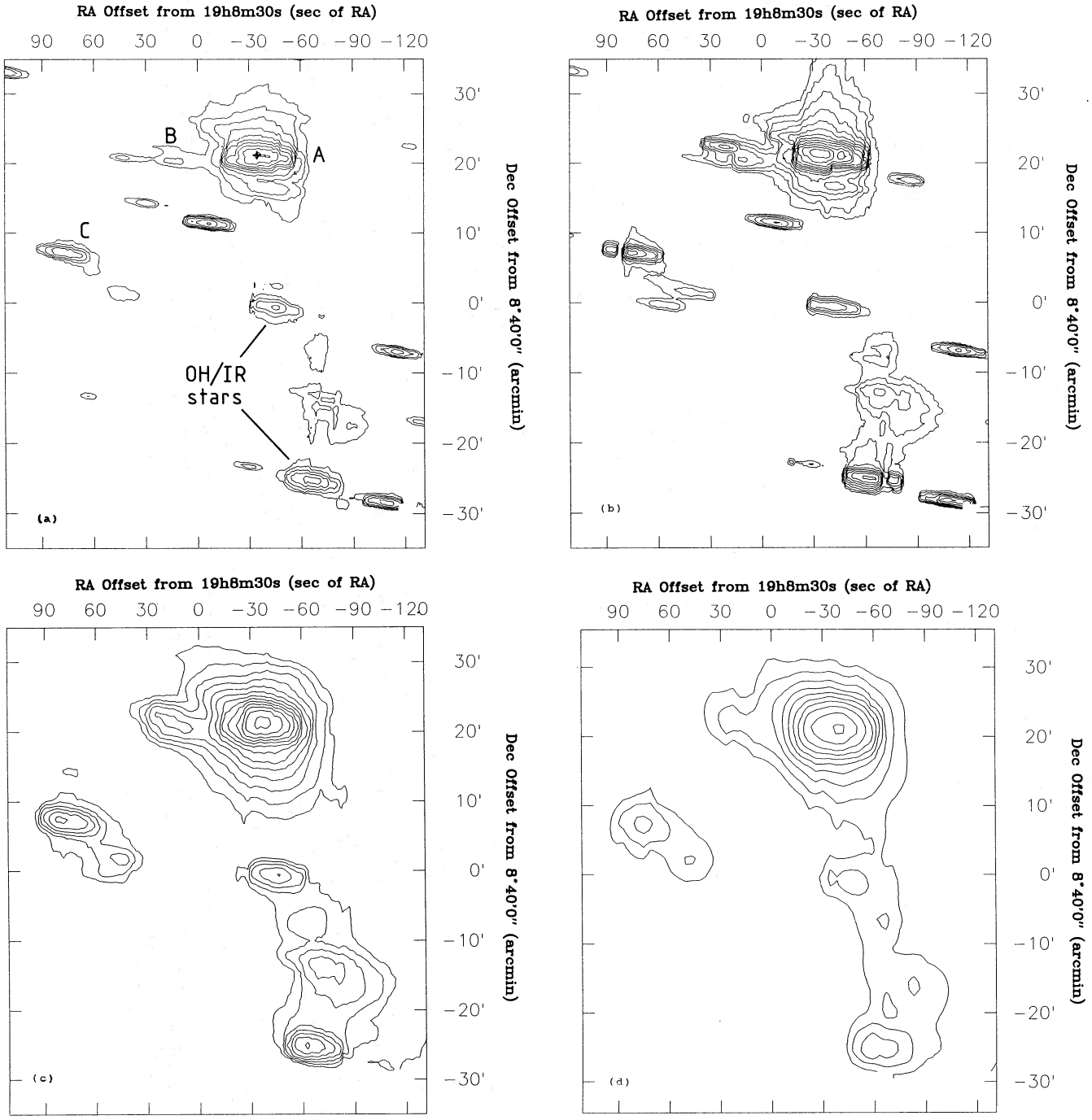

Figure 1. Isophotal contour maps of *IRAS* 19078+0901 (W49) at (a) 12 μm, (b) 25 μm, (c) 60 μm and (d) 100 μm. The reference position is: RA (1950) = $19^h 8^m 30\overset{s}{.}0$, Dec. (1950) = 8° 40′ 0″. Axes are marked in seconds of RA and arcmin, respectively. Base contours are: (a) 0.6, (b) 1.0, (c) 6.3 and (d) 25 Jy arcmin^{-2}, respectively. All contour intervals are 0.5 mag.

identified by the 20-arcsec resolution of the KAO observations of Harvey, Campbell & Hoffmann (1977). Nevertheless the peak *IRAS* contour at all four wavebands is located coincident with W49N, to within the positional accuracy of the two data sets.

The faint projection to the east of W49A, just visible at all four wavebands, is the supernova remnant W49B (Clegg, Rowan-Robinson & Ade 1976). The extended emission stretching almost a degree to the south of W49A, which is seen most clearly at 60 and 100 μm, consists of a number of foreground OH/IR stars: 42.3−0.2, 42.4−0.1, 42.4−0.2, OH42.60+0.07 and OH42.3−0.1 (Fix & Mutel 1984; Hauser *et al.* 1984; Herman *et al.* 1984; Caux *et al.* 1985; Gehrz *et al.* 1985). These sources are apparently connected by lower intensity emission, which has not been observed before to the best of our knowledge. Its *IRAS* fluxes give a colour temperature of 30–40 K and therefore is probably galactic cirrus emission.

The object marked C on Fig. 1(a) is *IRAS* source 19097+0847, which is a foreground H II region, G43.18−0.52, lying at 4.6±1.1 kpc (Wink, Altenhoff & Mezger 1982). This object has been studied at 1.3 mm by Chini *et al.* (1986), who derived a dust temperature of 22 K (our data give $T\sim 30$ K). On the basis of all of these measurements, Antonopoulou & Pottasch (1987) deduced that the object must be excited by a star of spectral type O9. For the remainder of this paper we shall concentrate solely on W49A.

Fluxes of W49A were measured in a box defined around the Band 4 source profile, and are listed in Table 1. Gordon (1987) has taken the maps of Harvey, Campbell & Hoffmann (1977) and Erickson & Tokunaga (1980) and has integrated the total emission down to the background limit. Comparison with his results shows that the *IRAS* fluxes are some 20 per cent less than would be predicted. However, given the uncertainties in the fluxes, these data are in agreement at the 1σ level.

Fig. 2 shows a 5–25 μm spectrum of W49A taken from the *IRAS* LRS catalogue. This is the averaged spectrum taken from the three Hours-Confirmed scans (HCONs) which crossed the source. The low resolution spectrograph consisted of two sets of detectors ('red' and 'blue') which overlapped around 13 μm, and a single spectrum is obtained by merging the two. In this case the agreement between the two was very good. The absolute errors in calibration are quoted in the LRS catalogue to be 10–15 per cent, but errors in the shape of an individual spectrum are quoted at only 2–4 per cent. 1σ error bars are shown in Fig. 2, and the solid line is a parabolic fit to the continuum.

Table 1. Flux measurements of W49A taken from Figs 1 and 3.

λ/μm	Aperture/arcmin	F/Jy	±%
12	15×18	976	30
25	15×18	5292	30
60	15×18	48300	30
100	15×18	82000	30
350	4×3	5500	40
800	4×3	403	40
1100	4×3	185	40
350	63″diam	2500	30
800	63″diam	178	30
1100	63″diam	63	30

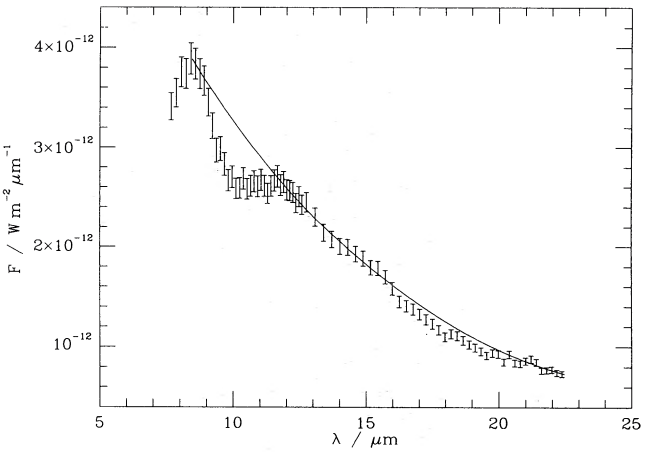

Figure 2. *IRAS* LRS spectrum of W49A. 1σ error bars are shown. The solid line shows a parabolic fit to the continuum. See text for discussion.

This spectrum is classified in the LRS catalogue as main class 1 (featureless spectrum with continuum rising to the blue). However, a very clear absorption band can be seen in Fig. 2 centred around 10 μm. This is identified as the 9.7-μm silicate feature on the basis of its position and appearance, and therefore we believe a better classification is class 3 ('blue' continuum with silicate absorption). The optical depth of the absorption feature is

$$\tau_{9.7} = 0.21 \pm 0.05.$$

This is about a factor of 4 less than that obtained by Gillett *et al.* (1975) who used a small beam (22 arcsec diameter) centred on W49(OH). This suggests that our larger beam contains emission which dilutes the feature, producing a smaller optical depth, so the silicate absorption is probably only seen against a small fraction of the large *IRAS* point source.

There are also a number of datapoints in the spectrum, centred around 18 μm, which lie more than 1σ below the continuum. This is consistent with the 18-μm silicate absorption feature which is usually seen in association with the 9.7-μm feature. If we ascribe this region to an absorption band, its optical depth is

$$\tau_{18} \simeq 0.09 \pm 0.03.$$

This is consistent with the usual ratio (Draine & Lee 1984):

$$\tau_{9.7}/\tau_{18} \sim 2.5$$

agreeing with our identification, although this is only tentative due to the weakness of this feature and the uncertainty in the continuum level.

The continuum flux reaches a maximum at 8.5 μm, corresponding to a blackbody equivalent temperature of 350 K,

which is somewhat larger than the estimate of Gillett *et al.* (1975). However, the flux turnover is too sharp for a blackbody, and many LRS spectra show a similar turnover, casting some doubt on the first few short wavelength detectors. The significance of all of these results is discussed in Section 5.

4 SUBMILLIMETRE DATA

Fig. 3(a–c) shows isophotal contour maps of a smaller region around the peak of W49N at 350, 800 and 1100 μm. W49SE and W49SW were not mapped in the submillimetre due to time constraints. However, Gordon & Jewell (1987) failed to detect any 1.3-mm emission from these regions. No structure has been resolved at any of the wavelengths used, and so the source is clearly small compared to the UKIRT beam, even at 350 μm. This will be discussed further in Section 5. The peak of the emission is also roughly coincident with the centre of the CO outflow (Scoville *et al.* 1986).

The morphology and interrelation between the various sources is shown schematically in Fig. 4. *IRAS* has only resolved W49A from W49B, whereas our submillimetre observations have resolved W49N itself. This single submillimetre source contains the seven H II regions of Dreher *et al.* (1984), the CO outflow of Scoville *et al.* (1986), and all of the known OH masers, H_2O masers, radio sources and near-infrared sources of the region. This strongly suggests that W49N is the most active component of W49A.

Total fluxes of W49N detected at each wavelength were measured, and are listed in Table 1. The data are in close agreement with previous work (e.g. Westbrook *et al.* 1976; Clegg, Rowan-Robinson & Ade 1976), although Schloerb, Snell & Schwartz (1987) obtained a slightly larger value for

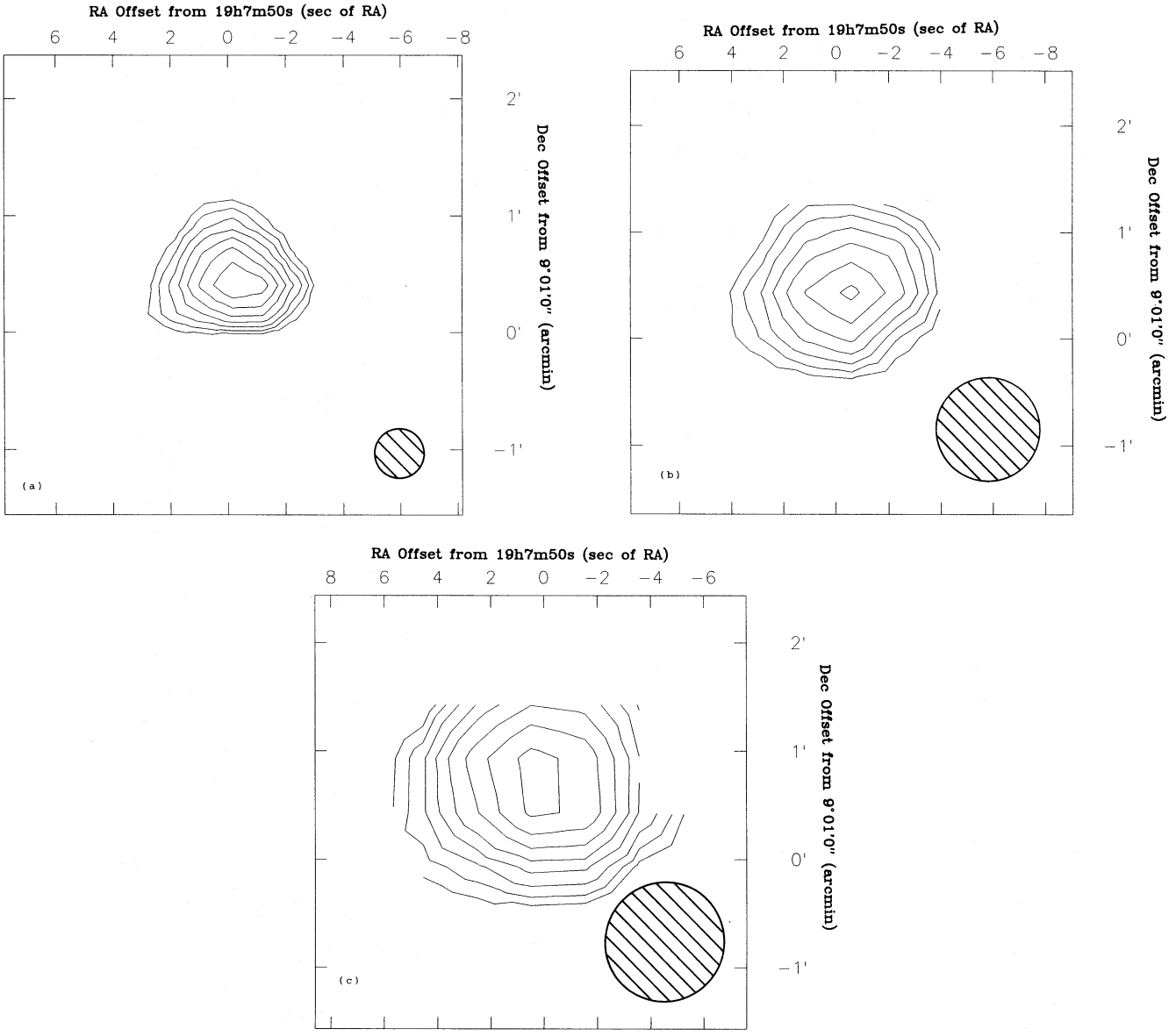

Figure 3. Isophotal contour maps of a smaller region around W49N at (a) 350 μm, (b) 800 μm and (c) 1100 μm. The reference position is: RA (1950) = $19^h7^m50\overset{s}{.}0$, Dec. (1950) = 9°01′0″. Beam sizes are shown as shaded circles. Axes are marked in seconds of RA and arcmin, respectively. Base contours are: (a) 38, (b) 16 and (c) 8 Jy arcmin^{-2}, respectively. All contour intervals are 0.5 mag.

the 1300-μm flux than Gordon (1987), indicating a somewhat lower submillimetre spectral index. Our data appear to lie somewhere between these two. Also listed in Table 1 are the results of single-point photometry in a 63-arcsec diameter aperture centred on the peak of W49N.

All the above data, apart from *IRAS*, were taken with telescopes utilizing chopping techniques. However, given that the 53-μm data of Harvey, Campbell & Hoffmann (1977) were obtained with a 5-arcmin chop, and that their map shows that W49N extends for less than 1 arcmin to the west of the peak, then the chop throw of 150 arcsec for our submillimetre data is sufficient to chop clear of the source, provided that the 53-μm and submillimetre data are measuring the same dust distribution.

The *IRAS* data provide an absolute upper limit to the source extent by virtue of the fact that it is unresolved by the *IRAS* detectors. Therefore a profile was taken through W49A in RA at 100 μm, and simulated submillimetre 'beams' placed at the separation of the chop throw. This provided a worst-case model for the fraction of the peak flux subtracted by the chop, which was found to be ~ 50 per cent. This must be a large overestimate, since other observations show that the source is considerably more compact than the *IRAS* resolution reveals (see discussion in Section 5).

At millimetre/submillimetre wavelengths it is possible that free–free emission might be significant. Gordon *et al.* (1986) mapped W49A at 3.5 millimetre, using a 70-arcsec aperture, and deduced that this was entirely free–free emission. Gordon (1987) used these data and found the free–free flux from W49N alone to be 8 Jy. The more recent 3-mm data of Salter *et al.* (1989) are consistent with this, and this value was used to compute and then subtract the free–free component from our 800- and 1100-μm fluxes prior to calculating the thermal emission spectrum. The free–free component was found to be insignificant at all shorter wavelengths. The physical consequences of all of these results are now addressed.

5 DISCUSSION OF THE DUST PARAMETERS

The emission from a greybody can be written (Gordon 1987) in the form

$$F_\nu = \Omega\, B_\nu(T)(1 - e^{-\tau}), \qquad (1)$$

where Ω is the solid angular extent of the emitting source in steradians, $B_\nu(T)$ is the blackbody emission at temperature T, and τ is the optical depth, such that

$$\tau = \left(\frac{\nu}{\nu_c}\right)^\beta, \qquad (2)$$

where β is the spectral index, and ν_c is the critical frequency at which the source becomes optically thin.

Fig. 5 shows our fluxes, corrected for free–free emission, plotted along with data taken from the literature (see figure caption). The solid curve represents a greybody which is seen to be consistent with most of the available data. The parameters of the fit are $T = 50$ K, $\beta = 1.8$, $\nu_c = 2000$ GHz ($\lambda_c = 150$ μm) and $\Omega = 1.5 \times 10^{-8}$ sr.

The infrared fluxes plotted in Fig. 5 were measured in an aperture which enclosed the whole of W49A, as discussed in Section 3, whereas the aperture used for the submillimetre

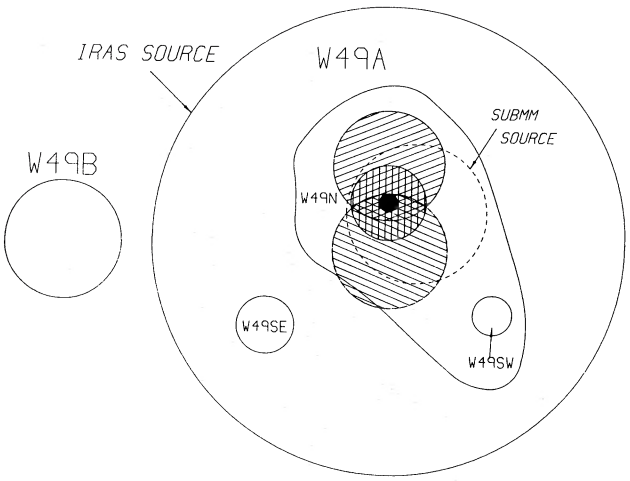

Figure 4. Schematic diagram of the morphology of W49 (not to scale). The diagonally shaded regions mark the CO outflow, the vertically shaded region is W49N and the solid region contains all of the H II regions and maser emission.

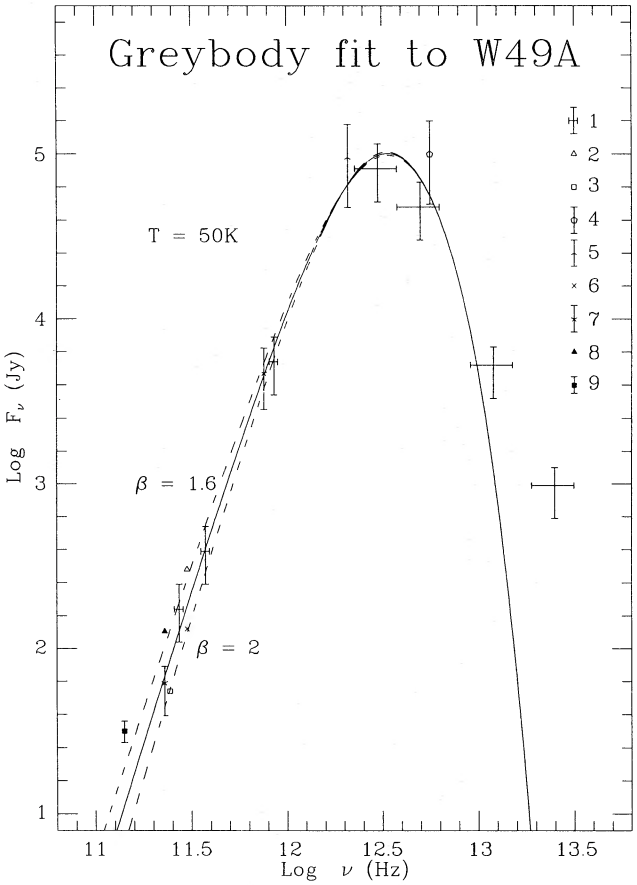

Figure 5. Compilation of all continuum fluxes of W49A available in the literature. The solid curve is a greybody fit to the data. The dashed curves show the effects of varying β. The symbols represent data taken from: (1) this paper; (2) Westbrook *et al.* 1976; (3) Clegg, Rowan-Robinson & Ade 1976; (4) Harvey, Campbell & Hoffmann 1977; (5) Erickson & Tokunaga 1980; (6) Chini *et al.* 1984; (7) Gordon 1987; (8) Schloerb, Snell & Schwartz 1987 and (9) Salter *et al.* 1989.

data only included W49N. The fact that the infrared and submillimetre data both lie on the same greybody curve shows that W49N is the dominant flux contributor to W49A in the infrared. Fig. 5 of Harvey, Campbell & Hoffmann (1977) is consistent with this observation.

The temperature and critical frequency used above agree with previous authors (although Herter *et al.* 1979 estimated a lower dust temperature), but the values of β and Ω are both somewhat less than was previously believed. The effects of varying β from 1.6 to 2.0 are illustrated by the two dashed lines in Fig. 5, showing that $\beta=2$ (Gordon 1987) is not inconsistent with the majority of the data, although our data and those of some other authors suggest a slightly lower value. This value of β is within the usually accepted range for dust clouds containing unmantled grains (Gear, Robson & Griffin 1988). The critical frequency can be used to estimate A_v (after Whitcomb *et al.* 1981), which is found to be ~1000 mag, a factor of 3 greater than the estimate of Westbrook *et al.* (1976).

The near-infrared continuum in Fig. 2 is redder than would be produced by a simple stellar spectrum, implying an additional component due to emission from warm dust. The excess emission at 12 μm seen in Fig. 5 supports this theory. A similar near-infrared excess has been observed before in Cepheus B (Evans *et al.* 1981), in infrared reflection nebulae (Leene 1986; Castelaz, Sellgren & Werner 1987), in the galactic cirrus emission (Weiland *et al.* 1986), and by ourselves in ρ Oph (Paper I). The usual explanation for this excess invokes an additional population of very small grains (VSGs), or even polycyclic aromatic hydrocarbons (PAHs), which are thermally spiked by individual photons (e.g. Puget 1987), and we suggest that this is occurring in W49A.

The total far-infrared luminosity of W49A can be calculated by integrating equation (1). The value obtained by performing this integration numerically (under the solid curve in Fig. 5) is $2.7\times10^7\ L_\odot$, slightly less than that found by Gordon (1987). The large value of A_v derived above means that all short wavelength emission from embedded stars is absorbed by the surrounding dust. This is then re-radiated in the infrared and submillimetre regimes. Thus our calculated luminosity is an estimate of the total luminosity of all embedded objects in the cloud (although it neglects the near-infrared excess).

Dreher *et al.* (1984) observed seven compact H II regions within W49N, in an area ~1 pc in diameter, and deduced that each must contain an O-type star. They derived a value for the total luminosity of these stars of $2.2\times10^6\ L_\odot$. This is consistent with our far-infrared luminosity since their estimate is a lower limit, not taking into account the possibility of a population of embedded low-mass stars contributing to the dust heating.

The critical frequency calculated above shows that at *IRAS* wavelengths the cloud is optically thick, so the infrared emission simply traces the dust distribution in the outer layers of the cloud, whereas the 800- and 1100-μm emission effectively samples dust at all depths. However, at the large distance of W49A it is not possible to resolve complex structure with our beam sizes.

The value of Ω deduced above implies a filling factor for the whole region which is only 75 per cent of the area of a single beam at 350 μm (the highest resolution of these data). This represents an effective diameter of the emitting region of ~2 pc. The evidence of previous work also suggests that the cloud is not uniform, but highly fragmented. For example, Dreher *et al.* (1984) argued that a uniform dust distribution could not explain the observed H II region emission, and that a clumpy morphology, possibly consisting partly of a series of shells around H II regions, was necessary to explain the results.

The mass of dust which is emitting in the submillimetre range (since the source has been shown to be optically thin in this range) can be calculated (Hildebrand 1983) from the equation

$$M_d=\frac{4a\rho D^2F_\nu}{3B_\nu(T)\,Q_\nu}, \qquad (3)$$

where a is the mean grain radius, ρ is the density of dust grain material, D is the distance to the cloud and Q_ν is the emissivity. Using typical values for each of the parameters, the total mass of dust was found to be 2400 $M_\odot\pm20$ per cent – in close agreement with Gordon (1987) and Mandolesi *et al.* (1984), but almost a factor of 2 less than the earlier estimate of Reifenstein *et al.* (1970).

This value of dust mass can be used to derive the number density of dust grains in W49A, assuming that the cloud has a similar length along the line-of-sight as in the other two dimensions. Using typical values for dust grain parameters we obtain a number density of 0.07 m^{-3}. The canonical value of 100 for the gas-to-dust mass ratio in dark clouds (Hildebrand 1983) leads to a cloud mass of $2.4\times10^5\ M_\odot$, consistent with the findings of Gillett *et al.* (1975).

All of our derived parameters for W49A are listed in Table 2. No errors are quoted due to the nature of the assumptions required to calculate some parameters. However, the values are all consistent with those found by Gordon (1987) except for the solid angle and the total infrared luminosity. These are both a factor of ~2 smaller than he found, due to the fact that the *IRAS* 60- and 100-μm fluxes are less than would be predicted from his 53- and 140-μm fluxes, so our greybody curve lies between the two extremes, and hence below Gordon's.

Table 2. Our derived parameters of W49A (see text for details).

Parameter	Value
T	50 K
β	1.8
Ω	0.18 arcmin^2
λ_c	150 μm
A_v	~1000 mag
M_d	2400 $M_\odot$
M_c	2.4×10^5 $M_\odot$
L_{IR}	2.7×10^7 $L_\odot$
L_{IR}/M_c	110 $M_\odot/L_\odot$
N_d	0.07 m^{-3}

Comparison of the parameters in Table 2 with the global properties of molecular clouds in the first galactic quadrant (Scoville & Good 1989) shows that the dust temperature in W49A is some 15–20 K larger than the mean value for clouds containing H II regions. The luminosity is an order of magnitude greater than the mean, as is the estimated luminosity-to-mass ratio of the cloud. This confirms that W49A is one of the most intrinsically luminous star-forming regions in the Galaxy.

Several conclusions can be drawn from the foregoing discussion. The mass and luminosity of the cloud, coupled with the observed filling factor, suggest an extremely luminous but highly fragmented region. The greybody curve fitted to the continuum of Fig. 5 shows that there is extensive emission from unmantled silicate grains at $T = 50$ K, and the absorption bands in Fig. 2 confirm this. However, the near-infrared excess of Fig. 5, and the non-stellar continuum of Fig. 2 are both evidence that there is also a population of small hot grains ($T \sim 350$ K). The two grain populations must be mixed at all depths within the cloud, or the small grains would not have been detected in the near-infrared.

So we propose the following morphology for W49A: a compact area containing seven H II regions, centrally heating a surrounding fragmented dust cloud of grains at two characteristic temperatures depending on size, possibly containing a population of low-mass stars, and in which star formation may still be occurring. Further work is clearly needed, and high-resolution, high-frequency mapping with JCMT, or submillimetre interferometry, may assist in understanding more fully the core structure of this complex region.

ACKNOWLEDGMENTS

The authors wish to thank D. S. Berry for much assistance in the production and explanation of new *IRAS* software. The staff of the *IRAS* Post-Mission Analysis Facility of the Rutherford Appleton Laboratory, and the staff of UKIRT are thanked for assistance during the acquisition of data. *IRAS* was developed and operated by the Netherlands Agency for Aerospace Programs, SERC and NASA. UKIRT is operated by the Royal Observatory, Edinburgh, on behalf of SERC, who are also gratefully acknowledged for funding the Lancashire Polytechnic minor node of STARLINK, and DWT's PDRA.

REFERENCES

Antonopoulou, E. & Pottasch, S. R., 1987. *Astr. Astrophys.*, **173,** 108.
Becklin, E. E., Neugebauer, G. & Wynn-Williams, C. G., 1973. *Astrophys. Lett.*, **13,** 147.
Castelaz, M. W., Sellgren, K. & Werner, M. W., 1987. *Astrophys. J.*, **313,** 853.
Caux, E., Puget, J. L., Serra, G., Gispert, R. & Ryter, C., 1985. *Astr. Astrophys.*, **144,** 37.
Chini, R., Kreysa, E., Mezger, P. G. & Gemund, H. P., 1986. *Astr. Astrophys.*, **154,** L8.
Clegg, P. E., Rowan-Robinson, M. & Ade, P. A. R., 1976. *Astr. J.*, **81,** 399.
Draine, B. T. & Lee, H. M., 1984. *Astrophys. J.*, **285,** 89.
Dreher, J. W., Johnston, K. J., Welch, W. J. & Walker, R. C., 1984. *Astrophys. J.*, **283,** 632.
Duncan, W. D., Robson, E. I., Ade, P. A. R., Griffin, M. J. & Sandell, G., 1990. *Mon. Not. R. astr. Soc.*, **243,** 126.
Erickson, E. F. & Tokunaga, A. T., 1980. *Astrophys. J.*, **238,** 596.
Evans, N. J., Becklin, E. E., Beichman, C., Gatley, I., Hildebrand, R. H., Keene, J., Slovak, M. H., Werner, M. W. & Whitcomb, S. E., 1981. *Astrophys. J.*, **244,** 115.
Fix, J. D. & Mutel, R. L., 1984. *Astr. J.*, **89,** 406.
Gaume, R. A. & Mutel, R. L., 1987. *Astrophys. J. Suppl.*, **65,** 193.
Gear, W. K., Robson, E. I. & Griffin, M. J., 1988. *Mon. Not. R. astr. Soc.*, **231,** 55P.
Gehrz, R. D., Kleinmann, S. G., Mason, S., Hackwell, J. A. & Grasdalen, G. L., 1985. *Astrophys. J.*, **290,** 296.
Genzel, R. *et al.*, 1978. *Astr. Astrophys.*, **66,** 13.
Gillett, F. C., Forrest, W. J., Merrill, K. M., Capps, R. W. & Soifer, B. T., 1975. *Astrophys. J.*, **200,** 609.
Gordon, M. A., 1987. *Astrophys. J.*, **316,** 258.
Gordon, M. A. & Jewell, P. R., 1987. *Astrophys. J.*, **323,** 766.
Gordon, M. A., Jewell, P. R., Kaftan-Kassim, M. A. & Salter, C. J., 1986. *Astrophys. J.*, **308,** 288.
Harvey, P. M., Campbell, M. F. & Hoffmann, W. F., 1977. *Astrophys. J.*, **211,** 786.
Hauser, M. G., Silverberg, R. F., Stier, M. T., Kelsall, T., Gezari, D. Y., Dwek, E., Walser, D., Mather, J. C. & Cheung, L. H., 1984. *Astrophys. J.*, **285,** 74.
Herman, J., Isaacman, R., Sargent, A. & Habing, H. J., 1984. *Astr. Astrophys.*, **139,** 171.
Herter, T., Duthie, J. G., Pipher, J. L. & Savedoff, M. P., 1979. *Astrophys. J.*, **234,** 897.
Hildebrand, R. H., 1983. *Q. J. R. astr. Soc.*, **24,** 267.
IRAS Exploratory Supplement, 1984. Eds Beichman, C. A. *et al.*, NASA RP-1190, Washington, D.C.
Leene, A., 1986. *Astr. Astrophys.*, **154,** 295.
Mandolesi, K. *et al.*, 1984. *Astr. Astrophys.*, **133,** 293.
Neugebauer, G. *et al.*, 1984. *Astrophys. J.*, **278,** L1.
Puget, J. L., 1987. In: *Comets to Cosmology,* 3rd *IRAS* Conference Proceedings, ed. Lawrence, A., Springer-Verlag, Heidelberg.
Reifenstein, E. C., Wilson, T. L., Burke, B. F., Mezger, P. G. & Altenhoff, W. J., 1970. *Astr. Astrophys.*, **4,** 357.
Salter, C. J., Emerson, D. T., Steppe, H. & Thum, C., 1989. *Astr. Astrophys.*, **225,** 167.
Schloerb, F. P., Snell, R. L. & Schwartz, P. R., 1987. *Astrophys. J.*, **319,** 426.
Scoville, N. Z. & Good, J. C., 1989. *Astrophys. J.*, **339,** 149.
Scoville, N. Z., Sargent, A. I., Sanders, D. B., Claussen, M. J., Masson, C. R., Lo, K. Y. & Phillips, T. G., 1986. *Astrophys. J.*, **303,** 416.
van Gorkom, J. H., Goss, W. M., Shaver, P. A., Schwartz, V. J. & Harten, R. H., 1980. *Astr. Astrophys.*, **89,** 150.
Ward-Thompson, D., Robson, E. I., Whittet, D. C. B., Gordon, M. A., Duncan, W. D. & Walther, D. M., 1989. *Mon. Not. R. astr. Soc.*, **241,** 119.
Weiland, J. L., Blitz, L., Dwek, E., Hauser, M. G., Magnani, L. & Rickard, L. J., 1986. *Astrophys. J.*, **306,** L101.
Westbrook, W. E., Werner, M. W., Elias, J. H., Gezari, D. Y., Hauser, M. G., Lo, K. Y. & Neugebauer, G., 1976. *Astrophys. J.*, **209,** 94.
Whitcomb, S. E., Gatley, I., Hildebrand, R. H., Keene, J., Sellgren, K. & Werner, M. W., 1981. *Astrophys. J.*, **246,** 416.
Wink, J. E., Altenhoff, W. J. & Mezger, P. G., 1982. *Astr. Astrophys.*, **108,** 227.
Wynn-Williams, C. G., 1971. *Mon. Not. R. astr. Soc.*, **151,** 397.